JACC: CARDIOVASCULAR IMAGING
VOL. ■, NO. ■, 2020
© 2020 PUBLISHED BY ELSEVIER ON BEHALF OF THE
AMERICAN COLLEGE OF CARDIOLOGY FOUNDATION

ORIGINAL RESEARCH

T_1 Mapping Tissue Heterogeneity Provides Improved Risk Stratification for ICDs without needing Gadolinium in Patients with Dilated Cardiomyopathy

Shiro Nakamori, MD,[a] Long H. Ngo, PhD,[a] Jennifer Rodriguez, BA,[a] Ulf Neisius, MD,[a] Warren J. Manning, MD,[a,b] Reza Nezafat, PhD[a]

ABSTRACT

OBJECTIVES This study sought to determine whether myocardial tissue heterogeneity scanned by native T_1 mapping could improve risk stratification in patients with nonischemic dilated cardiomyopathy (NICM) evaluated for primary prevention by ICD.

BACKGROUND The benefit of insertable cardiac-defibrillator (ICD) as primary prevention ICD in patients with NICM remains to be fully clarified.

METHODS A total of 115 NICM candidates for primary prevention and 55 healthy controls with similar distributions of age and sex were prospectively enrolled. Imaging was performed at 1.5-T using a protocol that included cine magnetic resonance for left ventricular function, late gadolinium enhancement (LGE) for focal scarring, and 5-slice native T_1 mapping for diffuse fibrosis and heterogeneity. The last method was assessed by mean absolute deviation of the segmental pixel-SD from the average pixel-SD (Mad-SD). The primary endpoint was a composite of appropriate ICD therapy and sudden cardiac death.

RESULTS During a median follow-up of 24 months, 13 patients (11%) experienced the primary endpoint. Dichotomized Mad-SD >0.24 provided a comparable outcome to the presence of LGE for the primary endpoint (annual event rate: 9.8% vs. 10.9%). The integration of Mad-SD to global native T_1 showed excellent arrhythmic event-free survival (annual event rate: 0%), and high sensitivity of 85% (95% confidence interval [CI]: 55% to 98%) and moderate specificity of 72% (95% CI: 62% to 80%), with a C-statistic of 0.76 (95% CI: 0.64 to 0.87), which was comparable to the presence, location, or extent of LGE in its ability to predict arrhythmic events.

CONCLUSIONS Combined myocardium tissue heterogeneity and interstitial fibrosis assessment by native T_1 mapping is an important predictor of ventricular tachycardia and ventricular fibrillation and provides additive risk stratification for primary prevention ICD in NICM patients without the need for gadolinium contrast. (J Am Coll Cardiol Img 2020;■:■–■)
© 2020 Published by Elsevier on behalf of the American College of Cardiology Foundation.

From the [a]Department of Medicine, Cardiovascular Division, Beth Israel Deaconess Medical Center and Harvard Medical School, Boston, Massachusetts; and [b]Radiology, Beth Israel Deaconess Medical Center and Harvard Medical School, Boston, Massachusetts. Supported by U.S. National Heart, Lung, and Blood Institute grant R01HL127015 and American Heart Association grant 15EIA22710040. Dr. Nakamori has received a scholarship from Mie University Foundation International. Dr. Nezafat has received U.S. National Institutes of Health grants 5R01HL129185, 5R01HL127015, and 1R01HL129157 and American Heart Association grant 15EIA22710040. All other authors have reported that they have no relationships relevant to the contents of this paper to disclose.

The authors attest they are in compliance with human studies committees and animal welfare regulations of the authors' institutions and Food and Drug Administration guidelines, including patient consent where appropriate. For more information, visit the *JACC: Cardiovascular Imaging* author instructions page.

Manuscript received October 16, 2019; revised manuscript received February 27, 2020, accepted March 27, 2020.

ISSN 1936-878X/$36.00 https://doi.org/10.1016/j.jcmg.2020.03.014

ABBREVIATIONS AND ACRONYMS

CMR = cardiovascular magnetic resonance

EF = ejection fraction

GBCA = gadolinium-based contrast agent

ICD = implantable cardioverter-defibrillator

LGE = late gadolinium enhancement

LV = left ventricle

Mad-SD = mean absolute deviation of the segmental pixel-standard deviation

NICM = nonischemic dilated cardiomyopathy

RV = right ventricle

SCD = sudden cardiac death

VF = ventricular fibrillation

VT = ventricular tachycardia

BACKGROUND

Use of the implantable cardioverter-defibrillator (ICD) is an established therapy for reducing mortality in patients with life-threating ventricular tachycardia and ventricular fibrillation (VT/VF) (1,2). Current guidelines for the use of ICD as a primary preventative emphasizes mainly reduced left ventricular (LV) ejection fraction (LVEF) (3,4), but only a small percentage of ICD recipients actually receive appropriate ICD therapy (5,6), resulting in increasing societal costs and patient morbidity. In addition, the benefit of ICD primary prevention in patients with nonischemic dilated cardiomyopathy (NICM) has yet to be clarified (7,8), although evidence of a benefit is greater in patients with ischemic cardiomyopathy. Therefore, improved risk stratification to identify patients with NICM who are most likely to benefit from ICD is an unmet clinical need.

Although LVEF provides an indirect measurement of arrhythmogenicity, assessment of the myocardial tissue substrate may improve risk stratification. Late gadolinium enhancement (LGE) cardiac magnetic resonance (CMR) is the gold standard for assessment of regional myocardial fibrosis and may help predict a substrate for VT/VF in both ischemic and nonischemic cardiac disorders (9–11). However, there are recent safety concerns regarding gadolinium-based contrast agent (GBCA) deposition in the brain and other organs, and GBCAs are contraindicated in patients with moderate-to-severe renal dysfunction, despite high prevalence of renal dysfunction in patients with chronic heart failure (12). More importantly, malignant arrhythmia could occur in patients without any evidence of scarring by LGE.

In recent studies by Puntmann et al. (13), native T_1 in the septal myocardium shows prognostic utility in nonischemic cardiac disorders. Chen et al. (14) demonstrates that increased native T_1 is useful for predicting appropriate ICD therapy in patient populations undergoing ICD insertion. However, in those studies, the primary endpoint has been all-cause mortality, or a heterogeneous patient population was evaluated. Thus, additional studies assessing the prognostic value of T_1 mapping for NICM are essential. Considering the mechanism of VT/VF, the present authors hypothesized that myocardial tissue heterogeneity might play an important role in the genesis of VT/VF. Recently, there have been several novel approaches to measure new imaging markers from native T_1 or T_2 maps which may provide diagnostic or prognostic values. The present authors have recently reported that native T_1 is useful for predicting ventricular arrhythmia in nonischemic cardiomyopathy (15). Baeßler et al. (16) showed the mean absolute deviation of the segmental pixel SD (Mad-SD) on T_2 mapping reflected the inhomogeneity of myocardial tissue due to inflammatory changes in acute myocarditis. Approaches based on texture analysis and radiomics have also been recently proposed to measure new imaging markers from native T_1 and T_2 (17). Therefore, these novel imaging markers such as Mad-SD may be useful in risk stratification of patients with nonischemic cardiomyopathies who are eligible for an ICD. Consequently, the present study aimed to assess whether myocardial tissue heterogeneity using native T_1 mapping provided incremental value to global T_1 value for prediction of future risk of VT/VF in candidates for an ICD.

METHODS

STUDY POPULATION. We prospectively recruited patients with NICM who were referred to both general cardiology and electrophysiology services and scheduled to receive a primary ICD or undergo electrophysiology study, or both, or ablation between January 2014 and January 2018. Exclusion criteria included: 1) an ischemic cause, defined as the presence of any epicardial coronary artery dimeter stenosis >70%, a history of myocardial infarction, or a subendocardium-based LGE pattern; 2) persistent atrial fibrillation; 3) any contraindications to CMR; and 4) patients under the age of 18. The study protocol was approved by the center's Institutional Review Board, and written informed consent was obtained from all study participants.

IMAGE ACQUISITION AND DATA ANALYSIS. All CMR images were acquired using a 1.5-T scanner (Achieva 1.5-T model, Philips Medical Systems, Best, the Netherlands) equipped with a 32-channel cardiac receiver coil. Cine image acquisition protocol and data analysis are provided in the Supplemental Appendix. Native T_1 was performed at 5 different slice locations covering the whole LV from base to apex by using the free-breathing slice-interleaved T_1 mapping

CENTRAL ILLUSTRATION **Combined Myocardium Tissue Heterogeneity and Interstitial Fibrosis Assessment by Native T_1 Mapping**

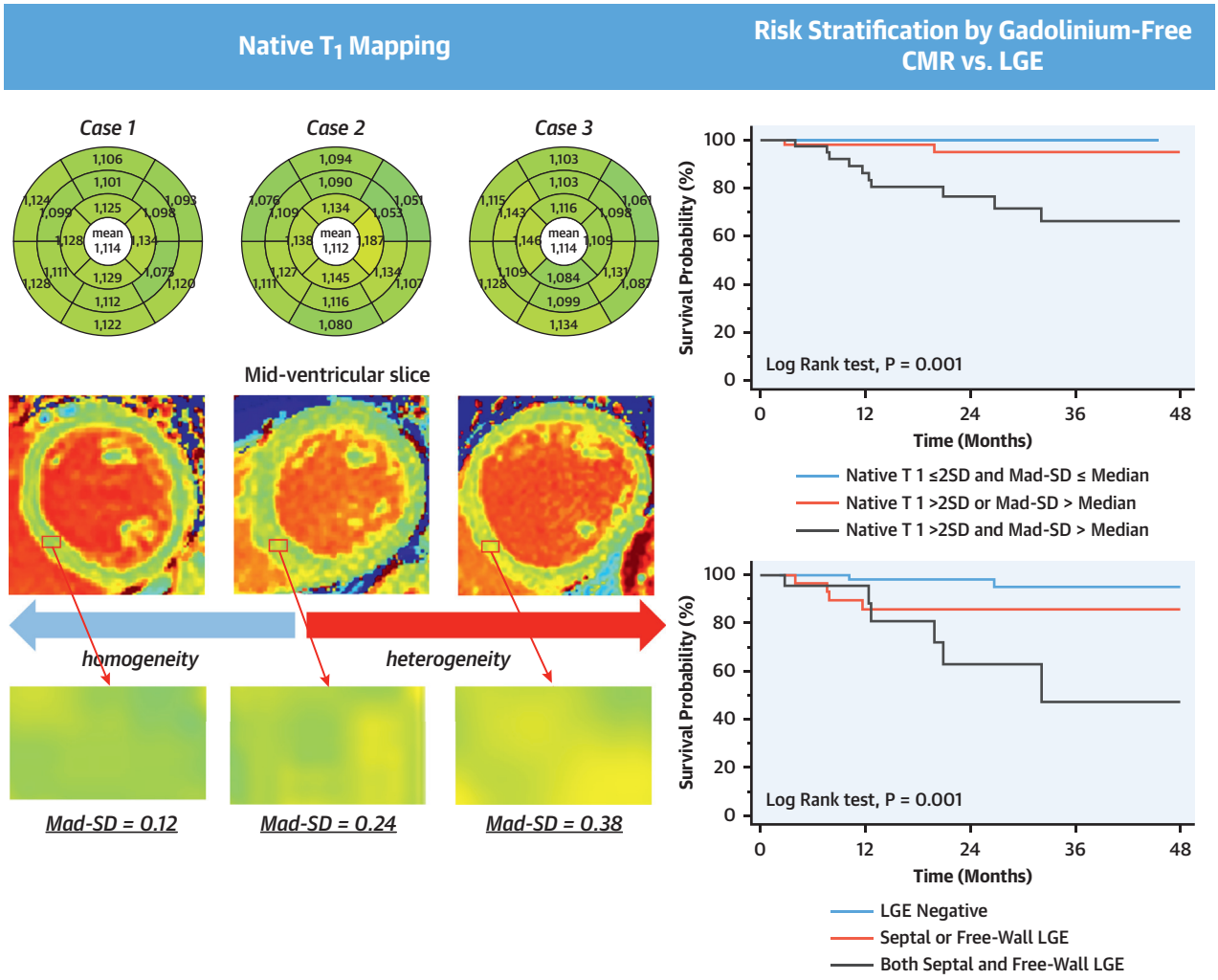

Nakamori, S. et al. J Am Coll Cardiol Img. 2020;■(■):■–■.

Mad-SD assessment on native T_1 mapping can represent various types of texture feature in the myocardium, and increased Mad-SD reflects myocardial tissue heterogeneity. The integration of Mad-SD into the native T_1 assessment is comparable to LGE in its ability to predict future VT/VF risk in NICM patients being considered for primary prevention ICD. ICD = implantable cardioverter-defibrillator; LGE = late gadolinium enhancement; Mad-SD = mean absolute deviation (of pixel) SD; NICM = nonischemic dilated cardiomyopathy; VF = ventricular fibrillation; VT = ventricular tachycardia.

sequence (see Supplemental Appendix). Segmental native T_1 values were measured over the 16 myocardial segments from 5 slices. Segments 1 to 6 were obtained from the most basal slice, whereas segmental T_1 values in segments 7 to 12 and 13 to 16 were calculated by averaging 2 mid-ventricular slices and 2 apical slices, respectively. Global native T_1 and maximum segmental native T_1 values were also computed. Standard deviations of all pixels within each myocardial segment were recorded as "segmental pixel-SD," and segments without ≥150 pixels were excluded for analysis. The maximum segmental pixel-SD (defined as the 1 segment of the 16 segments that exhibited the highest pixel SD) and global pixel-SD values were calculated. In order to assess myocardial tissue heterogeneity, the mean absolute deviation of the segmental pixel SD logarithmically transformed from the average on the transformed scale (Mad-SD) was computed using the following formula, as previously described, to assess

FIGURE 1 Types of Myocardial Tissue Heterogeneity in Patients With NICM and Similar Global Native T_1 Value

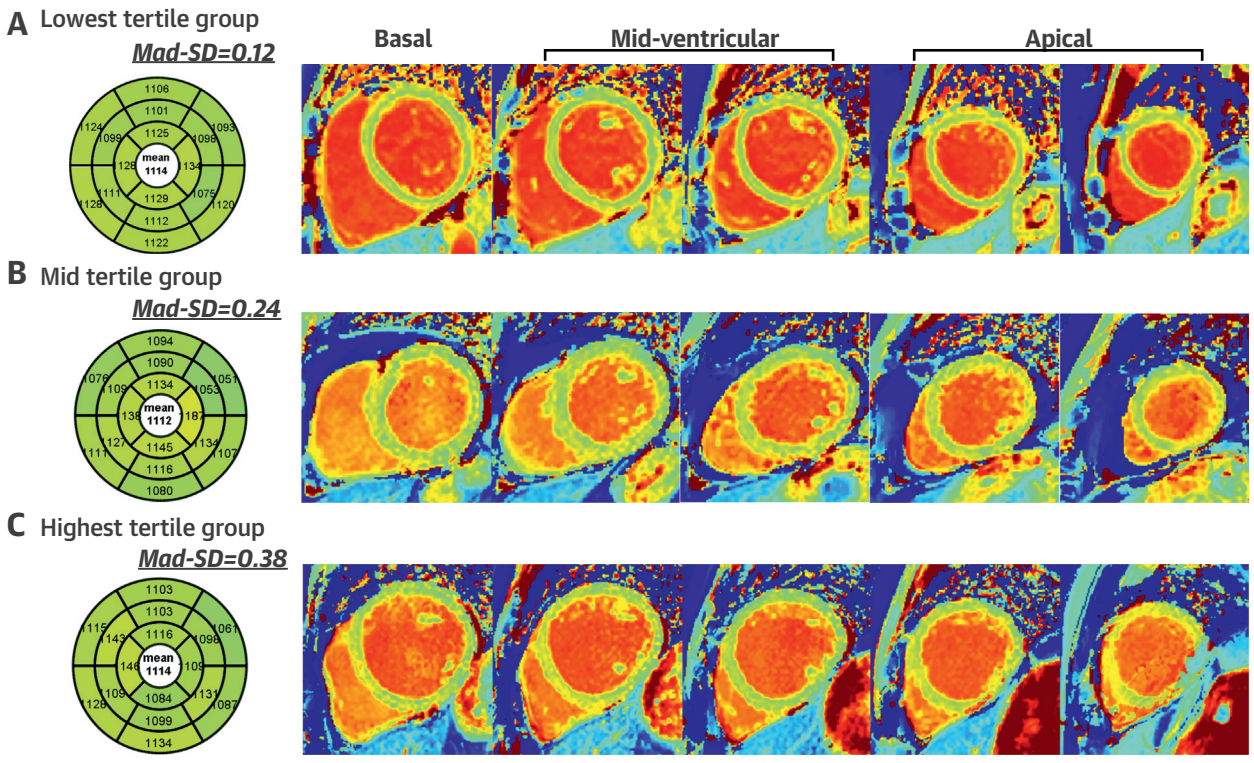

(A) The lowest tertile group presents with a smooth homogeneous profile in most parts of the myocardium, whereas **(C)** the highest tertile group is visually characterized by a patchy pattern predominantly in the basal slice. Examples **(A-C)** shown correspond to 0.12, 0.24, and 0.38 of the Mad-SD index, indicating that Mad-SD may be able to reflect myocardial tissue heterogeneity. Mad-SD = mean absolute deviation (of pixel) standard deviation; NICM = nonischemic dilated cardiomyopathy.

the inhomogeneity of myocardial edema on T_2 mapping (16):

$$Average\ Log^e\ Segmental\ pixel\ SD = \frac{\sum_1^{16} log^e\ Segmental\ pixel\ SD}{16}$$

$$Mad-SD = \frac{\sum_1^{16} |log^e\ Segmental\ pixel\ SD - Average\ log^e\ Segmental\ pixel\ SD|}{16}$$

To evaluate interobserver and intraobserver reproducibility, measurements of Mad-SD from a random sample of 10 patients with NICM were independently assessed by 2 observers, and 1 observer measured Mad-SD twice on 2 separate days with a washout period of at least 2 weeks. **Central Illustration and Figure 1** show representative cases with various types of myocardial tissue heterogeneity. For the septal native T_1, a region of interest of relatively large size of ≥150 pixels was placed on the septal myocardium at the mid-ventricular level without LGE enhancement, by avoiding contamination with the blood pool signal and artifact due to a misregistration error.

3-Dimensional (3D) LGE images were acquired 10 to 20 min after the patient received an injection of 0.1 to 0.2 mmol/kg of Gd-BOPTA (MultiHance, Bracco Imaging SpA, Milan, Italy) (see the Supplemental Appendix for imaging parameters and data analysis).

FOLLOW-UP. Patients were implanted with a conventional or a biventricular ICD device at the discretion of the implanting physician and without knowledge of native T_1 values. All devices were programmed for both antitachycardia pacing and shock with 3 zones of therapy including shock for VF, antitachycardia pacing followed by shock for fast VT, and a monitored zone for slower VT. Exact therapy settings were adjusted at the discretion of the implanting physician. Devices were interrogated at 1 and 3 months after implantation and every 6 months thereafter in the device clinic, and adjudication of stored ICD electrograms was performed by an

electrophysiologist blinded to CMR findings. The primary endpoints for this study were delivery of appropriate ICD therapy for VT/VF; hemodynamically unstable sustained VT/VF >30-s duration; or sudden cardiac death (SCD), defined as unexpected death from a cardiac cause that occurred within 1 h of symptom onset or within 24 h of last being observed in normal health.

STATISTICAL ANALYSIS. We computed the power analysis using the comparison of 2 conditional probabilities: the probability of having appropriate ICD/SCD, given that the patient belonged to the high level of Mad-SD category versus the probability of having appropriate ICD/SCD given that the patient belonged to the low Mad-SD category. These possibilities were estimated to be 30% versus 5%, respectively. With type I error of 0.05 and a power of 0.85, the required sample size was 80. We accounted for an attrition rate of up to 10%, which then brought the sample size to 90. Statistical analyses were performed using SPSS version 19 software (IBM, Armonk, New York) and R version 3.2.3 software (R Project, Vienna, Austria). Continuous variables are expressed as mean ± SD or median (quartiles) as appropriate and were compared using an unpaired Student *t*-test or a Mann-Whitney nonparametric *U* test if not normally distributed. Categorical variables were reported as counts and percentages and were compared using a chi-squared test or Fisher exact test if at least 1 of the expected cell counts was <5. Continuous variables were divided into tertiles. One-way ANOVA with Bonferroni adjustment for multiple comparisons was applied after the overall 3 group comparisons. Univariate Cox proportional hazards regression models were used to assess the association between each variable and the primary endpoint. For multivariate Cox proportional hazards modeling, the rule of thumb of having at least 5 outcomes per predictor was applied (18) and the 2 to 3 most significant variables from the univariable models were included. All associations reported in this study are hazard ratios (HR) and their corresponding 95% confidence intervals (CI). Kaplan-Meier curves were used to estimate the distribution of time to the first episode of appropriate ICD therapy, VT/VF, or SCD. Differences between time-to-event curves were compared using the log-rank test. The area under the receiver-operating characteristic curve was calculated and compared for all predictive tests for appropriate ICD/SCD. Intraobserver and interobserver reliability of Mad-SD measurements were assessed using the intraclass correlation coefficient.

The clinical risk score model was also calculated by using demographic, rhythm status, general cardiac status, and laboratory variables in the following formula: clinical risk score = −0.2 • age + 4 • male + 4 • nonsustained VT + 5 • atrial fibrillation − 8 • amiodarone + 4 • digoxin + 7 • pre-existing pacemaker − 3 • smoking − 0.2 • [QRS duration − 130] − 8 • anemia (defined as a hemoglobin concentration of <12 g/dl) + 1.77 • creatinine (19). All tests were 2-sided, and p values of <0.05 were considered significant. Subsequently, native T_1 and Mad-SD were integrated into the clinical risk model to assess improvement in discrimination of arrhythmic events. Reclassification of patients was determined by using net reclassification improvement analysis for appropriate ICD/SCD and obtained by adding Mad-SD status to the model based on native T_1. Because no conventional cutoff values exist for the onset of ICD therapy/SCD in such a population, risk categories were used to divide patients into low-risk (0% to <10%), low-intermediate risk (10% to <15%), high-intermediate risk (15% to <20%), and high risk (≥20%) categories. Categorical net reclassification improvement was computed together with integrated discrimination improvement.

RESULTS

PATIENT POPULATION. The baseline clinical characteristics of 115 patients with NICM (mean age: 54 years; 89 males [77%]) were separated into 3 tertiles and 55 healthy controls with similar age and sex distribution are shown in **Table 1**. At the time of the scans, 44% of patients were considered New York Heart Association (NYHA) functional class III; 83 of those patients (72%) received implantations of ICDs, generally during the evaluation; 34 days (interquartile range [IQR]: 7 to 94 days) after undergoing the CMR scan. The decision implant an ICD was guided by standard consensus criteria including LVEF and/or electrophysiology study results but was performed at the discretion of the treating physician after consultation with the patient. There was high usage of angiotensin-converting enzyme inhibitor/angiotensin receptor blockers, beta-blockers, and mineralocorticoid antagonists in this NICM patient population (92%, 95%, and 52%, respectively). The patients in the mid Mad-SD tertile group tended to be older, male, and have a higher prevalence of diabetic mellitus, whereas there was a trend toward higher NYHA functional class and N-terminal pro-B-type natriuretic peptide (NT-proBNP) in patients with higher Mad-SD scores (p = 0.22 and 0.23, respectively). There was no significant differences among

TABLE 1 Patient Clinical Characteristics

	Healthy Controls (n = 55)	NICM Patients (n = 115)	p Value	Lowest Mad-SD (n = 38)	Mid Mad-SD (n = 39)	Highest Mad-SD (n = 38)	p Value
Age, yrs	53 ± 5	54 ± 15	0.75	51 ± 16	57 ± 13	52 ± 16	0.25
Males	43 (78)	89 (77)	0.91	30 (79)	33 (85)	26 (68)	0.23
Body surface area, m^2	2.03 ± 0.22	2.03 ± 0.23	0.94	2.00 ± 0.22	2.07 ± 0.22	2.01 ± 0.23	0.35
Body mass index, kg/m^2	28.5 ± 4.7	28.8 ± 6.2	0.67	28.4 ± 5.9	29.4 ± 6.3	28.7 ± 6.6	0.80
Hypertension, %		40 (35)		12 (32)	14 (36)	14 (37)	0.88
Diabetes mellitus, %		20 (17)		5 (13)	11 (28)	4 (11)	0.09
Dyslipidemia, %		36 (31)		11 (29)	14 (36)	11 (29)	0.75
Smoking, %		12 (10)		3 (8)	5 (13)	4 (11)	0.78
History of stroke, %		6 (5)		1 (3)	3 (8)	2 (5)	0.61
Atrial fibrillation, %		17 (15)		6 (16)	7 (18)	4 (11)	0.64
COPD, %		3 (3)		1 (3)	1 (3)	1 (3)	>0.99
OSA, %		15 (13)		4 (11)	7 (18)	4 (11)	0.54
NYHA functional class							0.11
II		65 (56)		26 (68)	22 (56)	17 (45)	
III		50 (44)		12 (32)	17 (44)	21 (55)	
Received any ICD		83 (72)		29 (76)	27 (69)	27 (71)	0.77
Received biventricular ICD		22 (19)		7 (18)	9 (23)	6 (16)	0.71
Hemodynamics							
Systolic blood pressure, mm Hg	124 ± 15	113 ± 15	<0.001	115 ± 16	113 ± 12	111 ± 16	0.58
Diastolic blood pressure, mm Hg	74 ± 10	71 ± 13	0.13	72 ± 15	73 ± 10	69 ± 12	0.34
Heart rate, beats/min	63 ± 10	78 ± 17	<0.001	78 ± 16	76 ± 16	81 ± 18	0.38
Blood test							
Sodium, mmol/l		139 ± 3		139 ± 2	139 ± 3	138 ± 3	0.37
Blood urea nitrogen, mg/dl		19 ± 8		19 ± 10	19 ± 6	20 ± 8	0.85
Serum creatinine, mg/dl		1.03 ± 0.22		1.01 ± 0.18	1.05 ± 0.23	1.03 ± 0.24	0.74
Hemoglobin, g/dl		13.7 ± 1.9		13.9 ± 2.1	13.5 ± 1.8	13.6 ± 1.7	0.73
NT-proBNP, pmol/l		901 (492 to 2,146)		791 (386 to 1,668)	824 (484 to 2,090)	1,479 (625 to 4,181)	0.23
ECG parameter							
QRS duration, ms		115 ± 26		116 ± 27	114 ± 22	116 ± 29	0.92
Medication use							
ACE inhibitor or ARB		106 (92)		33 (87)	38 (97)	35 (92)	0.22
Beta-blocker		109 (95)		35 (92)	39 (100)	35 (92)	0.20
Mineralocorticoid antagonist		60 (52)		17 (45)	23 (59)	20 (53)	0.46
Amiodarone		11 (10)		4 (11)	3 (8)	4 (11)	0.89
Statin		53 (46)		16 (42)	20 (51)	17 (45)	0.71
Digoxin		21 (18)		6 (16)	6 (15)	9 (24)	0.57
Clinical risk score		5.7 (−1.8 to 10.7)		5.1 (−3.5 to 10.9)	6.5 (1.2 to 11.4)	6.1 (−0.7 to 8.8)	0.62
Length of follow-up, months		25 ± 19		24 ± 13	28 ± 26	24 ± 15	0.62

Values are mean ± SD, n (%), or median (interquartile range).

ACEI = angiotensin converting enzyme; ARB = angiotensin receptor blockers; COPD = chronic obstructive pulmonary disease; ECG = electrocardiography; ICD = implantable cardioverter-defibrillator; NICM = nonischemic dilated cardiomyopathy; NT-proBNP = N-terminal pro-B-type natriuretic peptide; NYHA = New York Heart Association; OSA = obstructive sleep apnea.

the clinical risk scores of the 3 groups. CMR characteristics for all groups are summarized in Table 2. Patients with NICM showed higher LV and RV cavities, higher LV mass indexes, and lower LV and RVEF (all $p < 0.01$), and a trend toward lower LV mass to LV end-diastolic volume ratio ($p = 0.11$). LGE was observed in 56 patients (49%). Mad-SD values and all native T_1 parameters were significantly higher in patients with NICM than in control subjects (0.27 ± 0.09 vs. 0.21 ± 0.04; $p < 0.001$). Figure 2 shows the distribution of NICM individuals shifts rightward toward higher Mad-SD. The cutoff Mad-SD values for the 3 NICM tertile groups were 0.22 and 0.28, respectively. Among the groups, patients in the mid Mad-SD tertile group were more likely to have a higher prevalence of LGE and higher septal and global native T_1. LV mass tended to be smaller at increasing Mad-SD values, resulting in LV mass to LV end-diastolic volume ratios and more eccentric remodeling in the highest Mad-SD group. Max segmental pixel-SD and max segmental native T_1 were higher in the highest Mad-SD group. In the segment-based analysis, 149 of 1,840 myocardial

TABLE 2 CMR Characteristics According to Myocardial Heterogeneity Tertile Category

	Healthy Controls (n = 55)	NICM Patients (n = 115)	p Value	Lowest Mad-SD (n = 38)	Mid Mad-SD (n = 39)	Highest Mad-SD (n = 38)	p Value
LV EDV, ml	158.7 ± 30.9	279.8 ± 94.3	<0.001	266.3 ± 87.5	283.6 ± 85.9	289.5 ± 108.5	0.54
LV EDVI, ml/m^2	78.1 ± 11.7	142.1 ± 41.6	<0.001	135.9 ± 43.2	140.6 ± 37.2	149.9 ± 44.1	0.38
LV ESV, ml	61.0 ± 15.6	203.7 ± 96.3	<0.001	188.3 ± 94.7	208.2 ± 83.3	214.9 ± 109.3	0.46
LV EF, %	61.8 ± 4.5	30.7 ± 15.9	<0.001	33.5 ± 17.9	29.0 ± 13.8	29.5 ± 15.9	0.40
LV EF <30%		68 (59)		20 (53)	24 (62)	24 (63)	0.60
LV mass, g	101.0 ± 25.2	154.2 ± 62.0	<0.001	156.1 ± 64.8	166.3 ± 69.2	140.4 ± 49.3	0.19
LV mass index, g/m^2	49.7 ± 10.7	75.5 ± 28.0	<0.001	76.5 ± 27.6	80.8 ± 33.7	69.2 ± 20.8	0.19
LV mass/LV EDV, g/ml	0.64 ± 0.16	0.59 ± 0.29	0.11	0.62 ± 0.29	0.63 ± 0.37	0.51 ± 0.14	0.13
LV LGE		56 (49)		14 (37)	24 (62)	18 (47)	0.09
LGE location							
Septal		38 (33)		10 (26)	15 (39)	13 (34)	0.25
Septal + free-wall		22 (19)		7 (18)	8 (21)	7 (18)	0.12
LGE pattern							0.20
Mid-wall		34 (30)		8 (21)	18 (46)	8 (21)	
Focal		6 (5)		2 (5)	2 (5)	2 (5)	
Epicardial		10 (9)		3 (8)	3 (8)	4 (11)	
Multiple		6 (5)		1 (3)	1 (3)	4 (11)	
LV LGE/LV mass, %		3.2 (2.1–6.2)		2.9 (2.1–6.1)	3.6 (2.4–5.9)	2.4 (1.6–7.1)	0.80
RV EDV, ml	158.1 ± 36.0	188.9 ± 65.4	<0.001	174.5 ± 58.3	197.2 ± 65.8	196.5 ± 71.7	0.27
RV EDVI, ml/m^2	78.0 ± 13.4	90.6 ± 28.2	0.001	85.6 ± 23.7	94.2 ± 31.9	92.2 ± 28.6	0.46
RV ESV, ml	64.7 ± 18.3	116.0 ± 63.8	<0.001	99.4 ± 55.3	123.5 ± 64.8	126.9 ± 69.5	0.16
RV EF, %	59.4 ± 5.4	42.2 ± 15.2	<0.001	46.6 ± 14.5	40.5 ± 14.4	39.1 ± 16.3	0.10
Mapping parameters							
Number of assessed segments		1,691 (92)		562 (92)	577 (92)	552 (91)	0.47
Septum native T_1, ms	1,067 ± 38	1,140 ± 55	<0.001	1,118 ± 52	1,153 ± 41	1,148 ± 68	0.01
Global native T_1, ms	1,067 ± 23	1,127 ± 44	<0.001	1,114 ± 38	1,137 ± 44	1,129 ± 48	0.08
Max segmental native T_1, ms	1,123 ± 34	1,204 ± 64	<0.001	1,184 ± 57	1,201 ± 50	1,229 ± 80	0.02
Global pixel-SD, ms	62 ± 9	72 ± 22	0.002	72 ± 26	70 ± 18	76 ± 22	0.30
Max segmental pixel-SD, ms	100 ± 21	111 ± 52	0.06	106 ± 44	116 ± 42	136 ± 36	0.004
Mad SD	0.21 ± 0.04	0.27 ± 0.09	<0.001	0.18 ± 0.03	0.24 ± 0.02	0.37 ± 0.07	<0.001
Septum ECV				0.30 ± 0.04	0.32 ± 0.09	0.32 ± 0.06	0.35
Global ECV				0.30 ± 0.04	0.33 ± 0.06	0.31 ± 0.06	0.15

Values are mean ± SD, n (%), or median (interquartile range).

ECV = extra-cellular volume fraction; EDV = end-diastolic volume; EDVI = end-diastolic volume index; EF = ejection fraction; ESV = end-systolic volume; ICD = implantable cardioverter-defibrillator; LGE = late gadolinium enhancement; LV = left ventricle; Mad = mean absolute deviation; RV = right ventricular; SD = standard deviation.

segments (8%) were excluded from cardiac and respiratory motions or incomplete registration due to poor image quality. LGE-positive segments (n = 178) showed higher segmental native T_1 values than LGE-negative segments (n = 1,513; 1,145 ± 54 ms vs. 1,124 ± 65 ms; p < 0.001). However, there were no differences in segmental pixel-SD between segments with and without LGE (72 ± 31 ms vs. 72 ± 33 ms, respectively; p = 0.64). The intraclass correlation coefficients for interobserver and intraobserver measurements of Mad-SD were 0.91 (95% CI: 0.70 to 0.98) and 0.97 (95% CI: 0.88 to 0.99), respectively.

ADVERSE EVENTS ACCORDING TO THE MAD-SD TERTILE GROUPS. The median follow-up time was 24 months (IQR: 13 to 37). No patients were lost to follow-up. The primary endpoint of appropriate ICD therapy or SCD occurred in 13 patients (11%): 12 received appropriate ICD therapy (including unstable VT/VF), and 1 experienced SCD (Table 3). The primary endpoint and appropriate ICD therapy alone significantly increased with increasing Mad-SD tertile and occurred more frequently in the highest Mad-SD group (primary endpoint: 0% vs. 13% vs. 21%, respectively; p = 0.01, appropriate ICD; 0% vs. 10% vs. 21%; p = 0.01). Eighteen patients had heart failure requiring hospitalization. There was a trend toward higher prevalence of heart failure hospitalization in the mid Mad-SD group but not in the highest Mad-SD group (lowest vs. mid vs. highest = 8% vs. 23% vs. 16%, respectively; p = 0.19).

PREDICTORS OF ARRHYTHMIC EVENTS. Univariate and multivariate Cox regression analyses of clinical and CMR parameters for the primary endpoint are summarized in Table 4. Among the

FIGURE 2 Distribution Pattern of the Mad-SD in Patients With NICM and Healthy Controls with Similar Age and Sex Distributions

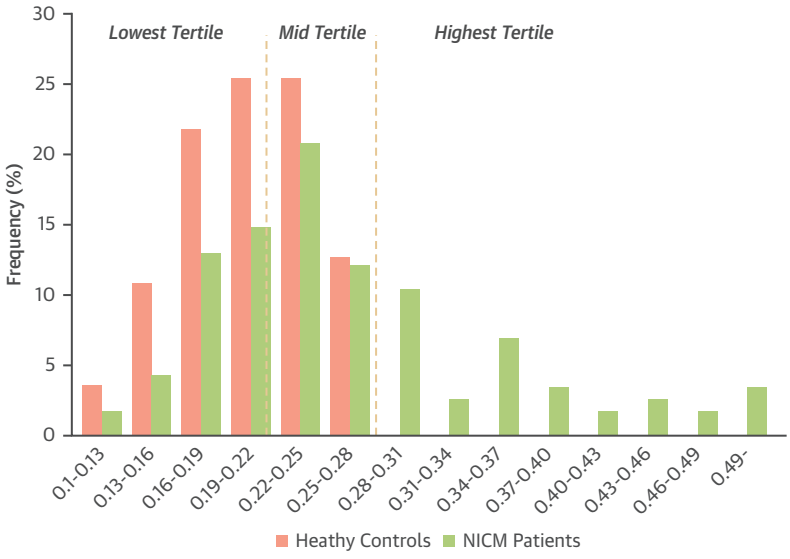

Based on 55 healthy controls whose Mad-SD ranged from 0.12 to 0.27, Mad-SD ≥0.27 was estimated to be abnormally elevated (beyond the 95th percentile, assuming a normal distribution). The distribution for NICM individuals shifted rightward toward higher Mad-SD. Abbreviations as in Figure 1.

clinical parameters, NYHA functional class III and increased creatinine levels were univariate predictors. Among the imaging parameters, the presence, septal location, and extent of LGE, reduced RVEF, global native T_1, and increased Mad-SD were significant predictors of arrhythmic events. Increased Mad-SD index remained associated with the onset of arrhythmic events, even after adjustment for the presence or location of LV LGE (Mad-SD tertile; HR: 4.49; 95% CI: 1.35 to 14.98; p = 0.01; HR: 4.15; 95% CI: 1.25 to 13.82; p = 0.02, respectively). In a simulated clinical decision making pathway using dichotomized variables, including native T_1 >2 SD (defined as mean ± 2 SD of global native T_1 from healthy controls) versus ≤2 SD and Mad-SD >0.24 (median) vs. Mad-SD ≤0.24, Mad-SD compared favorably with global native T_1 value for the occurrence of arrhythmic events (Figures 3A and 3B). The combination of Mad-SD with native T_1 provided a comparable outcome to the presence, extent, or location of LGE in predicting arrhythmic events (Figures 3C to 3F). In addition, Kaplan-Meier curves showed excellent cardiac event-free survival in patients with native T_1 ≤2 SD and Mad-SD ≤0.24 (annual event rate: 0%) (Figure 3C, Central Illustration). The C-statistics for the presence, extent, and location of LGE and native T_1 for

TABLE 3 Clinical Events

	All NICM Patients With NICM (N = 115)	Lowest Mad-SD (n = 38)	Mid Mad-SD (n = 39)	Highest Mad-SD (n = 38)	p Value
Arrhythmic events	13 (11)	0 (0)	5 (13)	8(21)	0.01
Appropriate ICD therapy (including unstable VT/VF)	12 (10)	0 (0)	4 (10)	8 (21)	0.01
Sudden cardiac death	1 (1)	0 (0)	1 (3)	0 (0)	0.37
Cardiac death	2 (2)	0 (0)	0 (0)	2 (5)	0.13
Non-cardiac death	4 (3)	1 (3)	1 (3)	2 (5)	0.76
Inappropriate ICD therapy	3 (3)	0 (0)	1 (3)	2 (5)	0.36
HF requiring hospitalization	18 (16)	3 (8)	9 (23)	6 (16)	0.19

Values are n (%).
HF = heart failure; ICD = implantable cardioverter-defibrillator; VT/VF = ventricular tachycardia/ventricular fibrillation.

TABLE 4 Univariate and Multivariate Cox Proportional Hazard Models for the Association With Appropriate ICD Therapy/SCD

	Univariable			Mutivariable Model 1			Multivariable Model 2			Multivariable Model 3		
	HR	95% CI	P Value	HR	95% CI	P Value	HR	95% CI	P Value	HR	95% CI	P Value
Age, yrs	1.00	0.96–1.04	0.89									
Age, ≥75 yrs	0.95	0.12–7.35	0.96									
Males	1.24	0.33–4.57	0.75									
Biventricular ICD	0.04	0.00–17.57	0.29									
Hypertension	0.40	0.09–1.83	0.24									
Diabetes mellitus	0.92	0.20–4.20	0.91									
AF	2.27	0.61–8.41	0.22									
Serum creatinine per 0.1 increase	1.25	1.01–1.55	0.04									
NYHA functional class ≥III	3.40	1.02–11.30	0.046									
QRS duration	0.99	0.96–1.01	0.28									
CMR parameters												
LV EDVI	1.01	1.00–1.03	0.13									
LV ESV	1.00	1.00–1.01	0.38									
LV EF per 1% decrement	1.03	0.98–1.08	0.25									
LV EF ≤35%	1.35	0.37–5.00	0.65									
LV mass index	0.99	0.97–1.02	0.51									
LV mass/LV EDV per 0.01 decrease	1.03	0.99–1.07	0.11									
LV LGE												
Presence of LGE	7.07	1.54–32.48	0.01	7.14	1.56–32.77	0.01	7.56	1.64–34.74	0.009			
Septal LGE (by location)	2.91	1.37–6.20	0.006									
Septal and free-wall LGE (by location)	3.64	1.65–8.03	0.001							3.11	1.55–6.22	0.001
LGE volume, per 1% increase	1.29	1.06–1.56	0.01									
LGE volume >3.24% (median)	2.21	1.09–4.45	0.03									
RV EDVI	1.02	1.00–1.05	0.03									
RV ESV	1.01	1.00–1.02	0.11									
RV EF per 1% decrement	1.04	1.00–1.09	0.04									
CMR mapping parameters	1.01	0.98–1.03	0.58									
Septum native T_1 per 10-ms increase	1.05	0.96–1.15	0.26									
Global native T_1 per 10-ms increase	1.14	1.00–1.30	0.04									
Global native T_1 >2 SD	6.64	0.86–51.50	0.07									
Max segmental native T_1 per 10-ms increase	1.05	0.97–1.13	0.21									
Global pixel-SD	1.01	0.99–1.03	0.56									
Max segmental pixel-SD	1.01	1.00–1.02	0.18									
Mad-SD per 0.01 increase	1.06	1.00–1.11	0.04	1.06	1.01–1.12	0.03						
Mad-SD >0.24 (median)	10.32	1.33–79.95	0.03									
Mad-SD tertile (highest)	4.11	1.24–13.64	0.02				4.49	1.35–14.98	0.01	4.15	1.25–13.82	0.02

Model 1 included LV LGE and Mad-SD. Model 2 included LV LGE and Mad-SD tertile. Model 3 included LV LGE location and Mad-SD tertile.
HR= hazard ratio (i.e., hazards of the presence of the characteristic to the reference (absence), or to the change of 1 U (continuous variable). Other abbreviations are as in Tables 1 and 2.

predicting appropriate ICD therapy/SCD were 0.70 (95% CI: 0.59 to 0.82), 0.73 (95% CI: 0.64 to 0.81), 0.76 (95% CI: 0.68 to 0.84), and 0.68 (95% CI: 0.56 to 0.81), respectively. When Mad-SD was combined with native T_1, a greater C-statistic was observed than when either variable was used individually (C-statistic = 0.76; 95% CI: 0.64 to 0.87; Delong' test: p = 0.16). Furthermore, the addition of Mad-SD to native T_1 yielded 5 correct (up) reclassifications and 3 incorrect (down) reclassifications in the 13 patients with appropriate ICD/SCD. Additionally, 49 correct (down) reclassifications and 17 incorrect (up) reclassifications occurred in the 102 patients who did not have appropriate ICD/SCD. Overall, integration of native T_1 and Mad-SD values provided improvement in risk stratification (net reclassification index [NRI] of 0.47; 95% CI: 0.03 to 0.91; p = 0.04). Addition of native T_1 and Mad-SD as a clinical risk score model consisting of demographics, rhythm status, general cardiac status, and laboratory variables provided further risk stratification (C-statistic = 0.79; 95% CI: 0.67 to 0.92; Delong's test; p = 0.03) (Figure 4).

FIGURE 3 **Kaplan-Meier Curves for CMR Parameters and Arrhythmic Events Including Appropriate ICD and SCD**

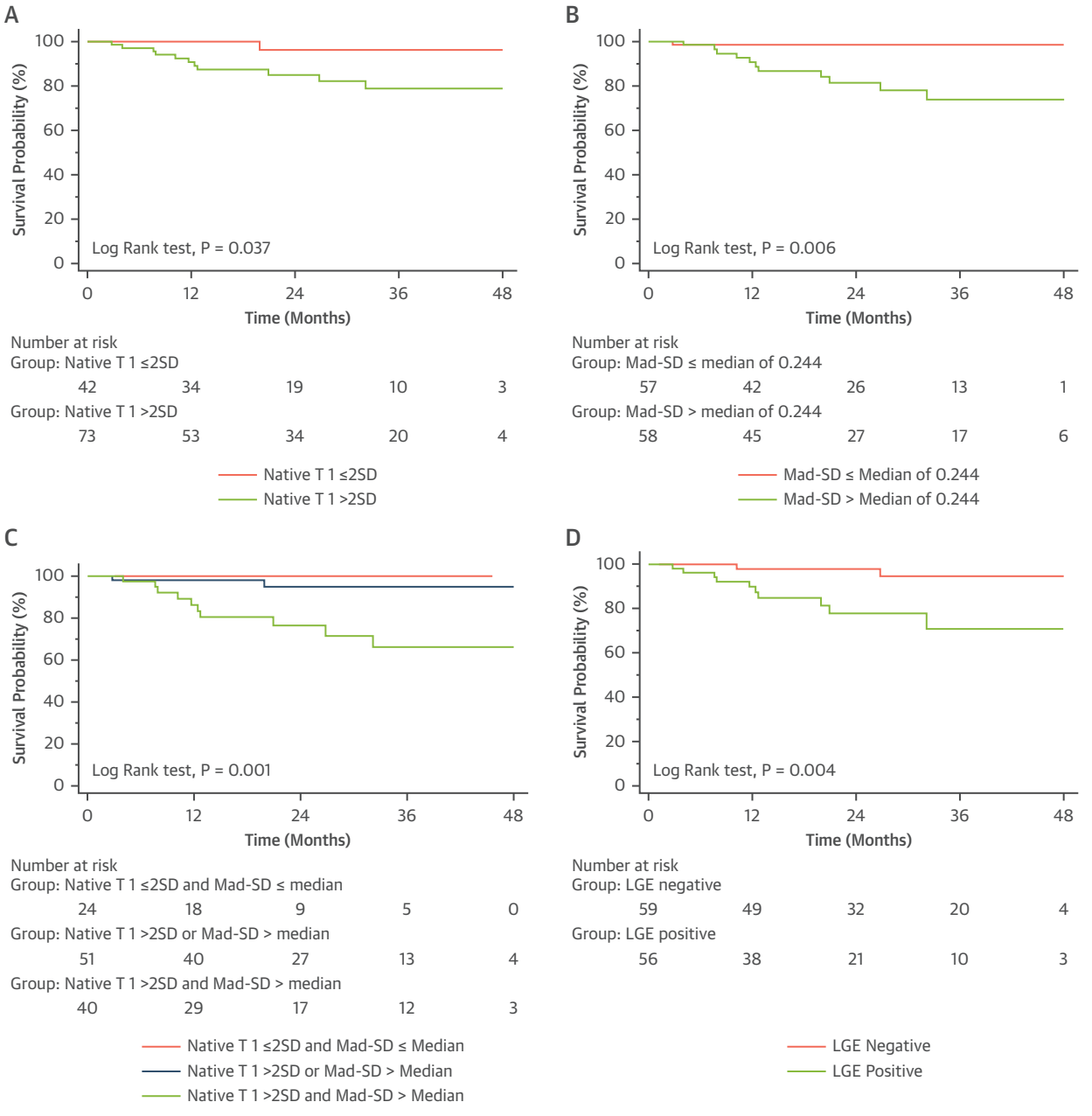

(A) Native T_1 >2 SD (defined as mean ± 2 SD of global native T_1 from healthy controls) versus ≤2 SD. **(B)** Mad-SD >median of 0.244 versus ≤median. **(C)** Native T_1 ≤2 SD and Mad-SD ≤0.244 versus native T_1 >2 SD or Mad-SD >0.244 versus native T_1 >2 SD and Mad-SD >0.244. **(D)** Present or absent LGE. **(E)** Absence of LGE versus LGE volume ≤ median of 3.24% versus >median. **(F)** Absence of LGE versus septal or free-wall LGE versus concomitant septal and free-wall LGE. LGE = late gadolinium enhancement.

Continued on the next page

FIGURE 3 Continued

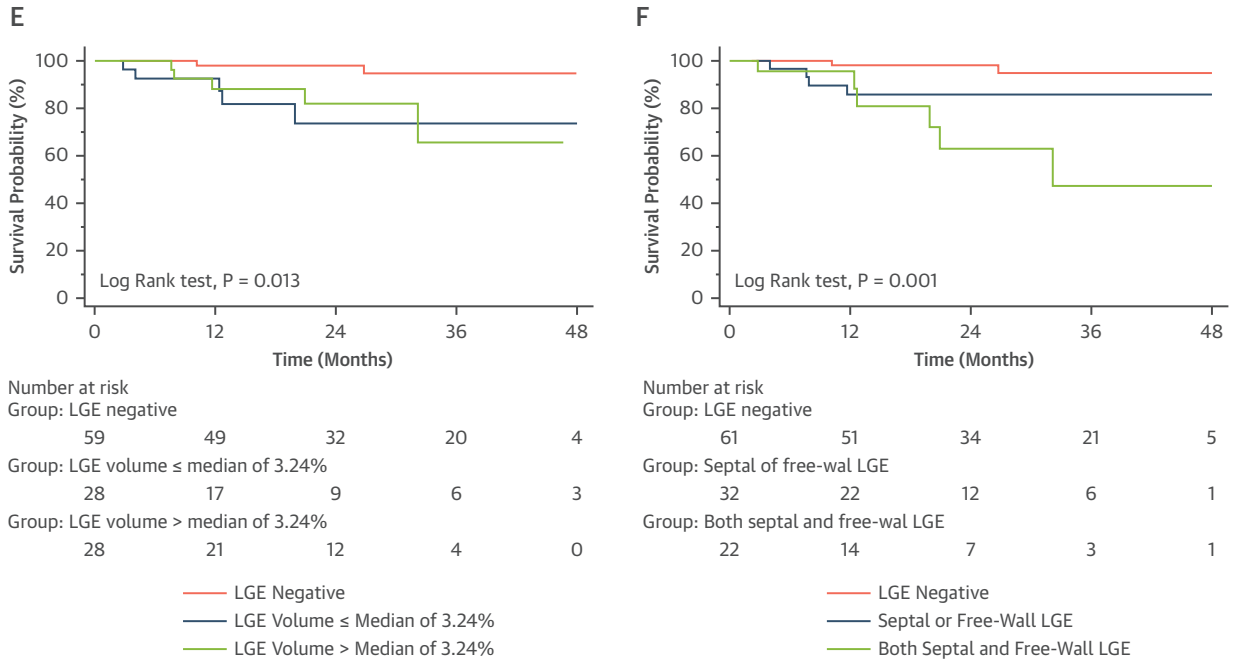

FIGURE 4 ROC Curves for Arrhythmic Events Including Appropriate ICD and SCD

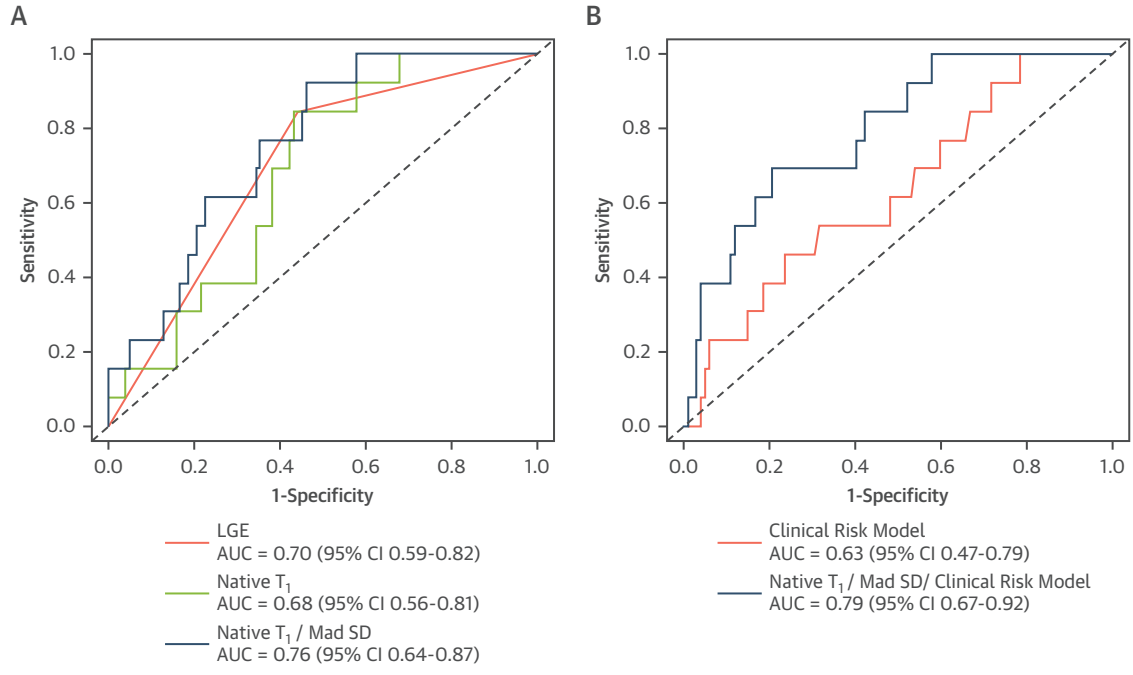

ROC curve and corresponding area under the curve describing the comparison of LGE, native T_1, native T_1, and Mad-SD to predict future arrhythmic events **(A)** and the incremental prognostic performance of native T_1 and Mad-SD for arrhythmic events beyond the clinical risk score model **(B)**. ICD = implantable cardioverter-defibrillator; ROC = receiver-operating characteristic; SCD = sudden cardiac death.

DISCUSSION

In this prospective study of 115 NICM candidates for primary prevention ICD implantation, we demonstrated that: 1) myocardial heterogeneity derived from Mad-SD is the important predictor of appropriate ICD/SCD beyond NYHA functional class and LVEF; 2) NICM patients with native T1 ≤2 SD and Mad-SD ≤0.24 showed excellent cardiac event-free survival; and 3) integration of Mad-SD into the global native T1 assessment is comparable to LGE in its ability to predict future VT/VF risk in patients with reduced LVEF being considered for primary prevention ICD therapy. Importantly, comprehensive native T_1 mapping assessment is useful for ruling out NICM patients with low risk of future VT/VF without the need for GBCA and may also eliminate the need for LGE CMR.

Currently, focal fibrosis by LGE is known to be associated with increased risk of VT/VF and adverse arrhythmic outcomes (9–11). In a subgroup analysis of systemic review and meta-analysis, the relationship between LGE and VT/VF was assessed in 421 patients with primary ICD from 5 observational studies. LGE was identified in 42% of patients, and the incidence of an arrhythmic event was 34% versus 4.5% in patients with and without LGE. LGE also provided an odds ratio of 7.8 for arrhythmic events (20). The results from our current study are consistent with those of previous studies, despite lower arrhythmic event rates. However, the potential link between GBCA and nephrogenic systemic fibrosis will limit the applicability of LGE CMR in patients with moderate-to-severe renal dysfunction, even if the ACR Committee on Drugs and Contrast Media considers the risk of nephrogenic systemic fibrosis in patients receiving standard or lower than standard doses of group II GBCAs is extremely low or possibly nonexistent.

Although the pathophysiology of post-infarct VT has been well described and relates to the propagation of a wave front around ventricular scar sustained by a re-entrant mechanism involving a "protected isthmus," the electrophysiological substrate for VT/VF in patients with NICM is not clearly defined. Studies have shown that diffuse myocardial fibrosis alters electric propagation between myocytes with potential proarrhythmic consequences in patients with NICM (21). Chen et al. (14) demonstrated that T_1 mapping was an independent predictor of appropriate ICD therapy. Due to a small sample size, no subgroup analysis could be performed despite the heterogeneity of the patient population. Furthermore, the imaging was limited to a single slice, which does not necessarily represent the myocardial characteristics of the whole myocardium. The association between global native T_1 at the 5-slice and appropriate ICD therapy/SCD were assessed. Although there were significant differences in global native T_1 between the NICM patients with and those without arrhythmic events, substantial overlap was found in T_1 values between them, which is similar to the authors' previous study and other study findings on cardiac T_1 mapping that discriminate between different patient cohorts based solely on myocardial T_1 values and hamper its clinical adoption (15,22). Indeed, the global native T_1 assessment showed a sensitivity of 92% and a specificity of 40% with an area under the curve of 0.68 for predicting arrhythmic events. This area under the curve value is slightly lower than the LGE assessment. However, combined assessment of global native T_1 and Mad-SD provides high sensitivity (85%) and moderate specificity (72%), with an area under the curve of 0.76 for arrhythmic events. That is, the combined assessment shows comparable performance to that of LGE CMR. Replacement fibrosis is one of several processes contributing to VT/VF. Studies have demonstrated that pathophysiological heterogeneity in cardiac tissue sustains VT, stabilizes re-entry VT, and provides substrate for VT/VF (23). The fibrosis microstructure and heterogeneity, not simply mass, may promote re-entry and result in sustained VT/VF by creating regions of conduction block with nonuniform anisotropy and slow conduction through diffuse and heterogeneous alterations in myocardial structure.

Currently, several vendors provide magnetic resonance-conditional ICDs, which may increase the applicability of myocardial tissue assessment even after cardiac device implantation. A recent study showed that, in most cases, CMR can offer diagnostic image quality for patients implanted with ICD (24). Given that GBCA retention is also related to the number of doses administered over time (25), repeated LGE CMR scans, particularly when closely spaced, need to be minimized or avoided. Native T_1 mapping can be derived without a need for GBCA and have the potential to follow serial changes in the myocardium over time and allow for a shorter imaging time and be useful for cost effectively identifying patients at risk for SCD. Combined assessment of interstitial fibrosis and its heterogeneity in the myocardial tissue might unveil new insights into assessment and stratification of patients with NICM being considered for ICD insertion. Large, multicenter studies are needed to confirm the NICM patient selection for primary ICD insertion based on parameters that can provide better risk stratification beyond LGE and current guidelines.

STUDY LIMITATIONS. The event rate was lower than had been anticipated when the study was designed, resulting in the study being underpowered (further details in the Supplemental Appendix). However, this CMR T_1 mapping study has the highest number of patients with NICM evaluated for primary ICD insertion. The present study is a proof-of-concept study with a small sample size. We took the small sample size issue into account in assessing variables included in the multivariable model. In Statistical Analysis, above, it was noted that a rule of thumb of having at least 5 outcomes per predictor and thus only considered 2 to 3 predictors for the multivariable model. Analysis focused on improving risk stratification in NICM candidates for primary prevention ICD and included patients without ICD who had refused the ICD despite being eligible for primary ICD insertion according to clinical guideline. Although those patients without an ICD had close follow-up examinations, receiving ambulatory electrocardiography monitoring or insertable cardiac monitor, some primary events might have been lost. Device choice and programming were not standardized and were left to the discretion of the operator. Mad-SD is not likely to be affected by subject variability, and segments with artifacts were carefully excluded. However, several imaging factors such as spatial resolution or blood partial volume effect could impact Mad-SD measurements. T_1 mapping with higher spatial resolution (26) or 3D T_1 mapping techniques (27–29) can potentially be used to improve the robustness of the measurements. Optimization of scan parameters and specific pulse sequence modifications designed to mitigate the impact of local field inhomogeneities on image quality are still needed to improve the success rate of CMR in patients with MRI-conditional ICDs. Also, further studies are needed to confirm the transferability of the Mad-SD measurement to other mapping sequences, field strengths or vendors.

CONCLUSIONS

This proof-of-concept study demonstrates that a combination of structural heterogeneity and interstitial fibrosis in the myocardial tissue may be an important predictor of VT/VF and provide additive risk stratification for primary prevention ICD in nonischemic patients with LV systolic dysfunction. Prospective, large multicenter studies are warranted to examine this comprehensive myocardial tissue characterization in the selection of patients for primary prevention ICD therapy.

ADDRESS FOR CORRESPONDENCE: Dr. Reza Nezafat, Department of Medicine, Cardiovascular Division, Beth Israel Deaconess Medical Center, 330 Brookline Avenue, Boston, Massachusetts 02215. E-mail: rnezafat@bidmc.harvard.edu.

PERSPECTIVES

COMPETENCY IN MEDICAL KNOWLEDGE: Myocardial heterogeneity derived from native T_1 map is the important predictor of appropriate ICD/SCD beyond NYHA functional class, LVEF, and LGE. Combined assessment of interstitial fibrosis and its heterogeneity from native T_1 map is comparable to LGE in its ability to predict future VT/VF risk in patients with reduced LVEF being considered for primary prevention ICD therapy.

TRANSLATIONAL OUTLOOK: We evaluated the feasibility of gadolinium free native T_1 tissue heterogeneity for additive risk stratification for primary prevention ICD in patients with NICM. Larger studies are warranted to confirm the utility of comprehensive native T_1 map assessment of interstitial fibrosis and structural heterogeneity in the myocardial tissue in the selection of patients for primary prevention ICD therapy.

REFERENCES

1. Antiarrhythmics versus Implantable Defibrillators (AVID) Investigators. A comparison of antiarrhythmic-drug therapy with implantable defibrillators in patients resuscitated from near-fatal ventricular arrhythmias. N Engl J Med 1997;337:1576–83.

2. Moss AJ, Zareba W, Hall WJ, et al., for the Multicenter Automatic Defibrillator Implantation Trial II investigators. Prophylactic implantation of a defibrillator in patients with myocardial infarction and reduced ejection fraction. N Engl J Med 2002;346:877–83.

3. Russo AM, Stainback RF, Bailey SR, et al. ACCF/HRS/AHA/ASE/HFSA/SCAI/SCCT/SCMR 2013 appropriate use criteria for implantable cardioverter-defibrillators and cardiac resynchronization therapy: a report of the American College of Cardiology Foundation appropriate use criteria task force, Heart Rhythm Society, American Heart Association, American Society of Echocardiography, Heart Failure Society of America, Society for Cardiovascular Angiography and Interventions, Society of Cardiovascular Computed Tomography, and Society for Cardiovascular Magnetic Resonance. J Am Coll Cardiol 2013;61:1318–68.

4. Priori SG, Blomström-Lundqvist C, Mazzanti A, et al. 2015 ESC Guidelines for the management of patients with ventricular arrhythmias and the prevention of sudden cardiac death: the Task Force for the Management of Patients with Ventricular Arrhythmias and the Prevention of Sudden Cardiac Death of the European Society of Cardiology (ESC). Endorsed by: Association for European Paediatric and Congenital Cardiology (AEPC). Eur Heart J 2015;36:2793–867.

5. Tung R, Zimetbaum P, Josephson ME. A critical appraisal of implantable cardioverter-defibrillator therapy for the prevention of sudden cardiac death. J Am Coll Cardiol 2008;52:1111–21.

6. Schmidt A, Azevedo CF, Cheng A, et al. Infarct tissue heterogeneity by magnetic resonance imaging identifies enhanced cardiac arrhythmia susceptibility in patients with left ventricular dysfunction. Circulation 2007;115:2006–14.

7. Kadish A, Dyer A, Daubert JP, et al., for the Defibrillators in Non-Ischemic Cardiomyopathy Treatment Evaluation (DEFINITE) investigators. Prophylactic defibrillator implantation in patients with nonischemic dilated cardiomyopathy. N Engl J Med 2004;350:2151–8.

8. Køber L, Thune JJ, Nielsen JC, et al., for the DANISH investigators. Defibrillator implantation in patients with nonischemic systolic heart failure. N Engl J Med 2016;375:1221–30.

9. Wu KC, Weiss RG, Thiemann DR, et al. Late gadolinium enhancement by cardiac magnetic resonance heralds an adverse prognosis in nonischemic cardiomyopathy. J Am Coll Cardiol 2008;51:2414–21.

10. Assomull RG, Prasad SK, Lyne J, et al. Cardiovascular magnetic resonance, fibrosis, and prognosis in dilated cardiomyopathy. J Am Coll Cardiol 2006;48:1977–85.

11. Gulati A, Jabbour A, Ismail TF, et al. Association of fibrosis with mortality and sudden cardiac death in patients with nonischemic dilated cardiomyopathy. JAMA 2013;309:896–908.

12. Marckmann P, Skov L, Rossen K, Dupont A, Damholt MB, Heaf JG. Nephrogenic systemic fibrosis: suspected causative role of gadodiamide used for contrast-enhanced magnetic resonance imaging. J Am Soc Nephrol 2006;17:2359–62.

13. Puntmann VO, Carr-White G, Jabbour A, et al. T1-mapping and outcome in nonischemic cardiomyopathy. J Am Coll Cardiol Img 2016;9:40–50.

14. Chen Z, Sohal M, Voigt T, et al. Myocardial tissue characterization by cardiac magnetic resonance imaging using T1 mapping predicts ventricular arrhythmia in ischemic and nonischemic cardiomyopathy patients with implantable cardioverter-defibrillators. Heart Rhythm 2015;12:792–801.

15. Nakamori S, Bui AH, Jang J, et al. Increased myocardial native T1 relaxation time in patients with nonischemic dilated cardiomyopathy with complex ventricular arrhythmia. J Magn Reson Imaging 2018;47:779–86.

16. Baeßler B, Schaarschmidt F, Dick A, et al. Mapping tissue inhomogeneity in acute myocarditis: a novel analytical approach to quantitative myocardial edema imaging by T2-mapping. J Cardiovasc Magn Reson 2015;17:115.

17. Neisius U, El-Rewaidy H, Nakamori S, Rodriguez J, Manning WJ, Nezafat R. Radiomic analysis of myocardial native T1 imaging discriminates between hypertensive heart disease and hypertrophic cardiomyopathy. J Am Coll Cardiol Img 2019;12:1946–54.

18. Stokes ME, Davis CS, Koch GG. Categorical Data Analysis Using SAS. 3rd Edition. Cary, NC: SAS Institute Inc., 2012.

19. Lee DS, Hardy J, Yee R, et al. Clinical risk stratification for primary prevention implantable cardioverter defibrillators. Circ Heart Fail 2015;8:927–37.

20. Di Marco A, Anguera I, Schmitt M, et al. Late gadolinium enhancement and the risk for ventricular arrhythmias or sudden death in dilated cardiomyopathy: systematic review and meta-analysis. J Am Coll Cardiol HF 2017;5:28–38.

21. Massare J, Berry JM, Luo X, et al. Diminished cardiac fibrosis in heart failure is associated with altered ventricular arrhythmia phenotype. J Cardiovasc Electrophysiol 2010;21:1031–7.

22. Puntmann VO, Voigt T, Chen Z, et al. Native T1 mapping in differentiation of normal myocardium from diffuse disease in hypertrophic and dilated cardiomyopathy. J Am Coll Cardiol Img 2013;6:475–84.

23. Pazó D, Kramer L, Pumir A, Kanani S, Efimov I, Krinsky V. Pinning force in active media. Phys Rev Lett 2004;93:168303.

24. Schwitter J, Gold MR, Al Fagih A, et al. Image quality of cardiac magnetic resonance imaging in patients with an implantable cardioverter defibrillator system designed for the magnetic resonance imaging environment. Circ Cardiovasc Imaging 2016;9. pii: e004025.

25. Roberts DR, Holden KR. Progressive increase of T1 signal intensity in the dentate nucleus and globus pallidus on unenhanced T1-weighted MR images in the pediatric brain exposed to multiple doses of gadolinium contrast. Brain Dev 2016;38:331–6.

26. Nezafat M, Ramos IT, Henningsson M, Protti A, Basha T, Botnar RM. Improved segmented modified Look-Locker inversion recovery T1 mapping sequence in mice. PLoS One 2017;12:e0187621.

27. Weingärtner S, Akçakaya M, Roujol S, et al. Free-breathing post-contrast three-dimensional T1 mapping: volumetric assessment of myocardial T1 values. Magn Reson Med 2015;73:214–22.

28. Weingärtner S, Akçakaya M, Roujol S, et al. Free-breathing combined three-dimensional phase sensitive late gadolinium enhancement and T1 mapping for myocardial tissue characterization. Magn Reson Med 2015;74:1032–41.

29. Mehta BB, Chen X, Bilchick KC, Salerno M, Epstein FH. Accelerated and navigator-gated look-locker imaging for cardiac T1 estimation (ANGIE): development and application to T1 mapping of the right ventricle. Magn Reson Med 2015;73:150–60.

KEY WORDS cardiac magnetic resonance, implantable cardioverter-defibrillator, native T_1, nonischemic dilated cardiomyopathy, tissue heterogeneity, ventricular fibrillation, ventricular tachycardia

APPENDIX For an expanded methods section, please see the supplemental version of this paper.